MethodsX 12 (2024) 102579

Contents lists available at ScienceDirect

MethodsX

journal homepage: www.elsevier.com/locate/methodsx

A mathematical model for investigation of dry band location on 22 kV bushing with and without RTV coating: Experimental study

L. Kalaivani [a], R.V. Maheswari [a], Emad Makki [b,*], Bharat Singh [c], Sanjay B Warkad [d], Jayant Giri [e], B. Vigneshwaran [a], Alagar karthick [f], Musaddak Maher Abdul Zahra [g], Abhinav kumar [h], Hitesh Panchal [i]

[a] Department of Electrical and Electronics Engineering, National Engineering College, Kovilpatti, 628503
[b] Department of Mechanical Engineering, College of Engineering and Architecture, Umm Al-Qura University, Makkah 24382, Saudi Arabia
[c] Department of Mechanical Engineering, GLA university, Mathura, India
[d] Department of Electrical Engineering, P R.Pote (Patil) College of Engineering & Management, Amravati 444603
[e] Department of mechanical Engineering, Yeshwantrao Chavan College of Engineering, Nagpur, India
[f] Renewable Energy Lab, Department of Electrical and Electronics Engineering, KPR Institute of Engineering and Technology, Coimbatore, 641407, Tamilnadu, India
[g] Computer Techniques Engineering Department, College of Engineering and Technologies, Al-Mustaqbal University, Babil, Iraq
[h] Department of Nuclear and Renewable Energy, Ural Federal University Named After the First President of Russia, Boris Yeltsin, 19 Mira Street, 620002, Ekaterinburg, Russia
[i] Gujarat Technological University Nr. Vishwakarma Government Engineering College Nr. Visat Three Roads, Visat - Gandhinagar Highway Chandkheda, Ahmedabad – 382424 - Gujarat, India

ARTICLE INFO

Method name:
Mathematical Model for investigating dry band location

Keywords:
Mathematical model
Numerical approach
ESDD
RTV coating
Solid layer method
Dry band

ABSTRACT

As different pollutants are deposited on the high voltage bushings, a dry band forms, which causes a flashover. The bushing's contaminated layer will weaken its insulation and have an impact on its electrical characteristics. The performance of bushings in dry band conditions of various lengths was investigated in this proposed piece of work, and a dynamic arc model is presented for the arc process in polluted bushings. It shows satisfactory performance in modelling the arc variables for various dry band positions. The developed dynamic open model for contaminated bushings with and without RTV coating predicted the flashover voltage and dry band positions. Any type of contamination, such as sea salt, road salt, and industrial pollutants prevalent in several sites, can be studied using the established model. Ultimately, it was discovered that there was good agreement between the model's results and the outcomes of the experiments.

- Mathematical modeling of 22 kV bushing is conceded out for diverse polluted dry band location at lead-in, lead-out and middle region of bushing surface.
- Dynamic arc modeling involved in bushing flashover process for different dry band location is done and flashover voltage is predicted
- Experimental work is carried out to find FOV for the bushing with different dry location and compared with predicted FOV.

* Corresponding author.
E-mail address: eamakki@uqu.edu.sa (E. Makki).

https://doi.org/10.1016/j.mex.2024.102579
Received 1 September 2023; Accepted 22 January 2024
Available online 26 January 2024

Specifications table

Subject area:	Engineering
More specific subject area:	Mathematical Modelling
Name of your method:	Mathematical Model for investigating dry band location
Name and reference of original method:	The methods and techniques used are in High Voltage Power Apparatus and the relevant references have been referred whenever needed
Resource availability:	This Method has been developed in MATLAB

Introduction

Bushings are designed for insulating the power transformer for indoor and outdoor applications. It is an insulated device that allows the safe passage of electrical energy through an earthed wall. High voltage (HV) bushing must get operated in various pollution, hot, cold, ambient, corrosive, and aggressive environmental conditions. When the bushings experience different atmospheric conditions, the pollutants get deposited on the surface of the bushings. This leads to dry band formation on the surface of the bushing and undergoes a flashover mechanism [1].

Bushings are often made of porcelain-type ceramic materials. To endure the greater voltages and thwart surface erosion and cracking, the porcelain components are covered with a glaze. In many substations, the insulators, bushings, and lightning arresters have typically been built with porcelain housings. Several research projects on high voltage insulators have been described by different scholars [2–5]. Comparing porcelain bushing to polymeric bushings, porcelain bushing offers greater self-cleaning qualities. When compared to composite bushings, porcelain bushings feature robust chemical connections that resist ageing and have a long lifespan. It is also simple to find the problem with porcelain bushings through visual investigation [6].

The severity of these polluted bushings relies on the deposition of bird secretions, natural dust, industrial contaminants, coastal salt, drizzle, and dew [7]. Hence, in order to determine the level of pollution and the variables affecting the performance of the pollution, the flashover performance of polluted bushings must be studied [8]. Pollutants that have built up on the surface of the bushing throughout the course of its use do not conduct when the surface is dry.It turns into a conductive layer when it's moist, which may be what starts the leakage current [9,10]. When the voltage stress across the dry band is greater than the withstand capacity, an arc may form. If the arc develops and flashover occurs frequently, the materials' dielectric strength is reduced [11].

In order to assess the dielectric strength under polluted conditions, fake pollution testing was conducted to examine the pollution behaviors on bushing surfaces. The most often utilized parameters for condition monitoring of HV bushings are the Equivalent Salt Deposit Density (ESDD), Surface Conductance, Leakage Current, Air Pollution Measurements, Optical Measurements, and the Non-soluble Deposit Density (NSDD) [12]. At the start of the arc's development, the magnitude of flashover voltage grew marginally, and it dramatically increased when flashover really occurred. When the bushing is clean, the electric field component is vertical as opposed to an overhead insulator, which results in a sliding sort of discharge.

The solubility of the materials accounts for the variation in performance of the naturally and intentionally contaminated insulators, even with the same ESDD. The contamination flashover voltage is significantly influenced by the surrounding temperature [13]. Moreover, the insulator configuration influences how well it performs during a flashover, so altering that configuration can raise the flashover voltage [14]. Although hydrophobic polymer insulators often exhibit excellent contamination withstand voltage properties, a major lowering of withstand voltage can occasionally occur under rapid and intense wetting and contamination conditions [15].

During the flashover process, electrical field lines were confined in the dry band. When electric field intensity was high, discharge started and it either covers partially or fully the surface of the bushing. The zero passage of alternating current (AC) current waveform occurred before total flashover resulted in arc extinction. The restriking of arc was reformed after satisfying the reigniting condition [16–19]. Effectively influencing the flashover process is the dry band formation. To forecast the flashover voltage under dry band conditions, an arc model is investigated. The flashover rises as a result of incomplete arcs [20–22].

In this paper, dynamic modeling of HV bushing discharge under polluted conditions is done by a passive component of an electrical network for different configurations such as pollution at lead-in region, lead-out region, and middle region of a 22 kV bushing with and without RTV coating. Initially, the electrical component values are determined to describe the static stable model of the bushing. The unstable flashover process of a bushing is then described using an extension of the static model, which can be used to calculate the temperature, propagation velocity, leakage current, linear resistance, length and radius of the arc, and temperature. The findings of the experimental procedure carried out in accordance with International Electro Technical Commission (IEC) 60507, solid layer pollution method, are then compared to the estimated flashover voltage and leakage current results.

The structure of this work is as follows. The mathematical modelling of high voltage bushing for lead-in, lead-out, and middle region single dry band creation as a result of pollution is covered in Section 2. Part 3 describes the experimental work linked to a single dry band of HV bushing and provides a flowchart of the suggested work included in the dynamic arc modelling. Section 4 contains the findings and discussion. The paper is concluded in Section 5.

Mathematical modeling

For insulators, a variety of models, including static and dynamic models, have been put out to explain the pollutant flashover process and forecast the flashover voltage [23,24]. The Obenaus model is a static model that takes into account an arc in series with resistance [22,25,26], whereas dynamic models take into account an arc as time-dependent and an impedance made out of an RLC

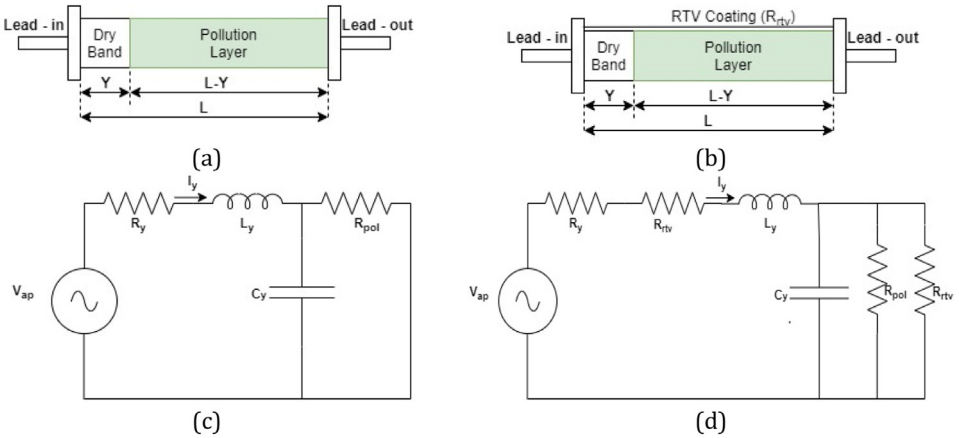

Fig. 1. Single dry band near lead-in region of HV bushing (a) without RTV coating (b) with RTV coating (c) Electrical equivalent circuit without RTV coating (d) Electrical equivalent circuit with RTV coating.

circuit [27]. The creation of dry bands and the association between dry bandwidth and temperature were studied by Salthouse [28]. This study takes into account contaminated bushing with single arc dry band formation on the surface close to the lead-in region, lead-out region, and middle region.

Single dry band near lead-in region

The high electric field intensity at the electrode ends causes a mathematical model for bushing with a single dry band to form close to the lead-in region due to pollution. The mathematical model for bushing having a single dry band near the lead-in region due to pollution is formed near the electrode ends due to high electric field intensity at those regions. Fig. 1(a) and 1(b) illustrate a schematic representation of a rectangular bushing sample without RTV coating and a single dry band in series with pollution layer, respectively (b). Fig. 1(c) and 1(d) demonstrate the electrical equivalent circuit for a single dry band close to the Lead-in region with and without RTV coating.

This dynamic model consist of applied power frequency AC voltage $V_{ap}(t)$,arcresistance (R_y), arc inductance (L_y), arc capacitance (C_y), pollution layer resistance (R_{pol}). The value of arc resistance depends on discharge length which is a function of time which is expressed in Eq. (1) [11,29]. The relationship between different circuit elements aids in finding the arc characteristics. The arc resistance can be calculated using Mayor's Equation [30] which is given by Eq. (1).

$$\frac{dR_y}{dt} = \frac{R_y}{\tau}\left(1 - R_y\frac{I_y^2}{A}\right) \tag{1}$$

where I_y = Arc current, τ = Arc time constant, A = Dynamic arc constant, R_y= Discharge resistance, y = Discharge length. The values 100μs is time constant and 10,000 is dynamic arc constant respectively [31].The inductance involved is calculated using Eq. (2) in [32,33].

$$L_y = \frac{\mu_0}{2\pi}\left[0.25 + \ln\left(\frac{y}{r_d}\right)\right] \tag{2}$$

Where r_d is the discharge radius calculated using Eq. (3) is then used in Eq. (4) for calculating the capacitance value of the discharge path.

$$rd = \sqrt{\frac{I_y}{1.45\pi}} \tag{3}$$

The discharge channel capacitance is calculated by using Eq. (4) [34].

$$C_y = 2\pi\varepsilon\alpha_y\left[1 + \left(\frac{r_d}{L - y}\right)\right] \tag{4}$$

Where α_y is calculated using Eq. (5)

$$\alpha_y = 1 - 1/\sqrt{1 + \left[\left(\frac{w}{2L}\right)\left(\frac{1}{1 - \left(\frac{y}{L}\right)}\right)\right]^2} \tag{5}$$

where w is the width of the pollution. Wilkins model [24] is used to evaluate the (R_{pol}) using Eq. (6) for narrow band.

$$R_{pol} = \frac{1}{2\pi\sigma}\left[\frac{\pi(L-y)}{\mathrm{w}} + \log\left(\frac{\mathrm{w}}{2\pi \mathrm{r_d}}\right)\right] \tag{6}$$

Eq. (7) is used to calculate (R_{pol}) for wide band.

$$R_{pol} = \frac{1}{2\pi\sigma}\left(\log\frac{2\mathrm{L}}{\pi \mathrm{r_d}} - \log\tan\frac{\pi \mathrm{y}}{2\mathrm{L}}\right) \tag{7}$$

The insulation resistance is therefore calculated using Eq. (8)

$$\mathrm{R_{rtv}} = \frac{\rho}{2\pi \mathrm{l}}.\ln(\mathrm{R_{rtv}}/\mathrm{r_d}) \tag{8}$$

The discharge current and flashover voltage are modeled using the state-space equation using Eq. (9).

$$\frac{\mathrm{dx}}{\mathrm{dt}} = \mathrm{Ax} + \mathrm{Bu} \tag{9}$$

Eqs. (10) and (11) are the voltage and current governing equation for electrical equivalent circuit for lead-in dry band position without RTV coating.

$$V_{ap}(t) = I_y(t)R_y(y,t) + L_y\frac{dI_y(t)}{dt} + V_c(t) \tag{10}$$

$$I_y(t) = C_y\frac{dV_c(t)}{dt} - \frac{V_c(t)}{R_{pol}(y,t)} \tag{11}$$

Eq. (12) shows the state-space equation for polluted bushing without RTV coating.

$$\begin{bmatrix}\frac{\mathrm{dI_y}}{\mathrm{dt}}\\ \frac{\mathrm{dV_c}}{\mathrm{dt}}\end{bmatrix} = \begin{bmatrix}-\frac{\mathrm{R_y}}{\mathrm{L_y}} & -\frac{1}{\mathrm{L_y}}\\ \frac{1}{\mathrm{c_y}} & \frac{1}{\mathrm{R_{pol}C_y}}\end{bmatrix}\begin{bmatrix}\mathrm{I_y}\\ \mathrm{V_C}\end{bmatrix} + \begin{bmatrix}\frac{\mathrm{V_{ap}}}{\mathrm{L_y}}\\ 0\end{bmatrix} \tag{12}$$

Eqs. (13) and (14) are the voltage and current governing equation for electrical equivalent circuit for lead-in dry band position without RTV coating.

$$V_{ap}(t) = I_y(t)R_y(y,t) + L_y\frac{dI_y(t)}{dt} + V_c(t) \tag{13}$$

$$I_y(t) = C_y\frac{dV_c(t)}{dt} - \frac{V_c(t)\left(R_{rtv} + R_{pol}(y,t)\right)}{R_{rtv} * R_{pol}(y,t)} \tag{14}$$

Eq. (15) shows the state-space equation for polluted bushing with RTV coating.

$$\begin{bmatrix}\frac{\mathrm{dI_y}}{\mathrm{dt}}\\ \frac{\mathrm{dV_c}}{\mathrm{dt}}\end{bmatrix} = \begin{bmatrix}\frac{-R_y - \mathrm{R_{rtv}}}{\mathrm{L_y}} & -\frac{1}{\mathrm{L_y}}\\ \frac{1}{\mathrm{c_y}} & \frac{1}{(\mathrm{R_{rtv}} + R_{pol})\mathrm{C_y}}\end{bmatrix}\begin{bmatrix}\mathrm{I_y}\\ \mathrm{V_C}\end{bmatrix} + \begin{bmatrix}\frac{\mathrm{V_{ap}}}{\mathrm{L_y}}\\ 0\end{bmatrix} \tag{15}$$

Single dry band near lead-out region

Due to the intensified electric field, the dry band forms close to the lead-out zone. Fig. 2(a) depicts the creation of a dry band close to the lead-out region of a contaminated bushing without RTV coating, and Fig. 2(c) depicts the electrical equivalent circuit.Fig. 2(b) depicts the creation of a dry band close to the lead-out region of a dirty bushing with RTV coating, and Fig. 2(d) depicts the electrical equivalent circuit.

Eqs. (16) and (17) are the voltage and current governing equation without RTV coating, and Eqs. (19) and (20) are used to describe for RTV coated equivalent circuit. The equivalent circuit of pollution dry band formation near lead-out region of HV bushing without RTV coating is given by Eq. (18) and bushing with RV coating is given by Eq. (23).

$$V_{ap}(t) = R_{pol}(y,t)C_y\frac{dV_c(t)}{dt} - I_y(t)R_{pol}(y,t) + V_c(t) \tag{16}$$

$$V_c(t) = I_y(t)R_y(y,t) + L_y\frac{dI_y(t)}{dt} \tag{17}$$

$$\begin{bmatrix}\frac{\mathrm{dI_y}}{\mathrm{dt}}\\ \frac{\mathrm{dV_c}}{\mathrm{dt}}\end{bmatrix} = \begin{bmatrix}-\frac{\mathrm{R_y}}{\mathrm{L_y}} & \frac{1}{\mathrm{L_y}}\\ \frac{1}{\mathrm{c_y}} & -\frac{1}{\mathrm{R_{pol}C_y}}\end{bmatrix}\begin{bmatrix}\mathrm{I_y}\\ \mathrm{V_C}\end{bmatrix} + \begin{bmatrix}0\\ \frac{\mathrm{Vap}}{R_{pol}C_y}\end{bmatrix} \tag{18}$$

$$V_{ap}(t) = \frac{R_{pol}(y,t) * R_{rtv}}{R_{pol}(y,t) + R_{rtv}}C_y\frac{dV_c(t)}{dt} - I_y(t)\frac{R_{pol}(y,t) * R_{rtv}}{R_{pol}(y,t) + R_{rtv}} + V_c(t) \tag{19}$$

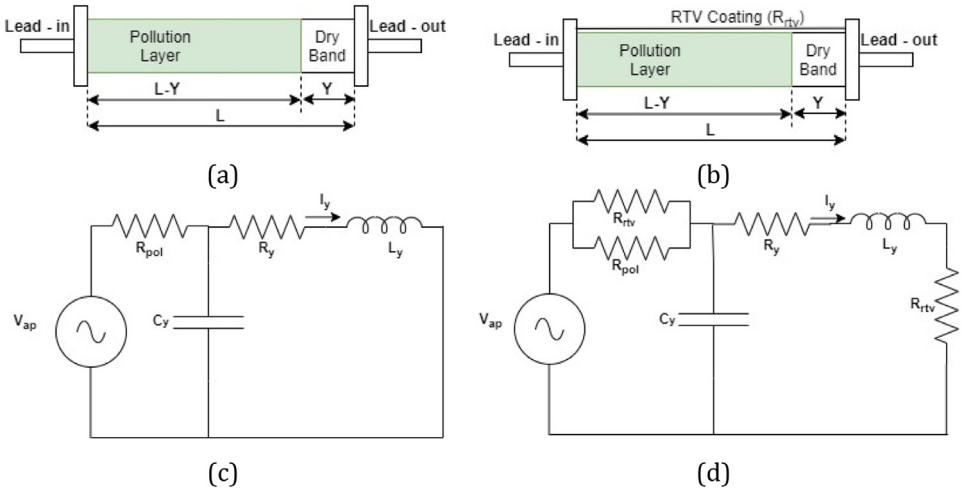

Fig. 2. Single dry band near lead-out region of HV bushing (a) without RTV coating (b) with RTV coating (c) Electrical equivalent circuit without RTV coating (d) Electrical equivalent circuit with RTV coating.

$$V_c(t) = I_y(t)(R_y(y,t) + R_{rtv}) + L_y \frac{dI_y(t)}{dt} \tag{20}$$

$$\begin{bmatrix} \frac{dI_y}{dt} \\ \frac{dV_C}{dt} \end{bmatrix} = \begin{bmatrix} -\frac{R_y+R_{rtv}}{L_y} & \frac{1}{L_y} \\ \frac{1}{C_y} & -\frac{R_{pol}+R_{rtv}}{R_{pol}*R_{rtv}*C_y} \end{bmatrix} \begin{bmatrix} I_y \\ V_C \end{bmatrix} + \begin{bmatrix} 0 \\ \frac{V_{ap}(R_{pol}+R_{rtv})}{R_{pol}*R_{rtv}*C_y} \end{bmatrix} \tag{21}$$

Single dry band in the middle region

Fig. 3(a) depicts the arrangement of a single dry band at the center of the HV bushing surface without RTV coating. This model can be visualized as a combination of two single arcs, and Fig. 3(c) depicts the electrical equivalent circuit. The electrical equivalent circuit of the bushing with a dry band placed in the middle of an RTV coated bushing is shown in Fig. 3(b) and 3(d). Eqs. (22–29) determine the calculation procedure of equivalent circuit parameters with and without RTV coating.

$$V_{ap}(t) = R_{pol1}(y,t)C_{y1}\frac{dV_{c1}(t)}{dt} - I_{y1}(t)R_{pol1}(y,t) + V_{c1}(t) \tag{22}$$

$$V_{c1}(t) = I_y(t)R_{y1}(y,t) + L_{y1}\frac{dI_y(t)}{dt} + I_y(t)R_{y2}(y,t) + L_{y2}\frac{dI_y(t)}{dt} + V_{c2}(t) \tag{23}$$

$$I_y(t) = C_{y2}\frac{dV_{c2}(t)}{dt} - \frac{V_{c2}(t)}{R_{pol2}(y,t)} \tag{24}$$

$$\begin{bmatrix} \frac{dI_y}{dt} \\ \frac{dV_{C1}}{dt} \\ \frac{dV_{C2}}{dt} \end{bmatrix} = \begin{bmatrix} -\frac{R_y}{L_y} & \frac{1}{L_y} & -\frac{1}{L_y} \\ \frac{1}{C_{y1}} & -\frac{1}{R_{pol1}C_{y1}} & 0 \\ \frac{1}{C_{y2}} & 0 & \frac{1}{R_{pol2}C_{y2}} \end{bmatrix} \begin{bmatrix} I_y \\ V_{C1} \\ V_{C2} \end{bmatrix} + \begin{bmatrix} 0 \\ \frac{V_{ap}}{R_{pol1}C_{y1}} \\ 0 \end{bmatrix} \tag{25}$$

$$V_{ap}(t) = \frac{R_{pol1}(y,t)*R_{rtv1}}{R_{pol1}(y,t)+R_{rtv1}}C_{y1}\frac{dV_{c1}(t)}{dt} - I_{y1}(t)\frac{R_{pol1}(y,t)*R_{rtv1}}{R_{pol1}(y,t)+R_{rtv1}} + V_{c1}(t) \tag{26}$$

$$V_{c1}(t) = I_y(t)(R_{y1}(y,t) + R_{rtv1}) + L_{y1}\frac{dI_y(t)}{dt} + I_y(t)\left(R_{y2}(y,t) + R_{rtv2}\right) + L_{y2}\frac{dI_y(t)}{dt} + V_{c2}(t) \tag{27}$$

$$I_y(t) = C_{y2}\frac{dV_{c2}(t)}{dt} - \frac{V_{c2}(t)\left(R_{pol2}(y,t)+R_{rtv2}\right)}{R_{pol2}(y,t)*R_{rtv2}} \tag{28}$$

$$\begin{bmatrix} \frac{dI_y}{dt} \\ \frac{dV_{C1}}{dt} \\ \frac{dV_{C2}}{dt} \end{bmatrix} = \begin{bmatrix} \frac{-R_y-R_{rtv1}-R_{rtv2}}{L_y} & \frac{1}{L_y} & -\frac{1}{L_y} \\ \frac{1}{C_{y1}} & -\frac{R_{pol1}(y,t)+R_{rtv1}}{R_{pol1}R_{rtv1}C_{y1}} & 0 \\ \frac{1}{C_{y2}} & 0 & \frac{(R_{pol2}+R_{rtv2})}{R_{pol2}R_{rtv2}C_{y2}} \end{bmatrix} \begin{bmatrix} I_y \\ V_{C1} \\ V_{C2} \end{bmatrix}]] + \begin{bmatrix} 0 \\ \frac{(R_{pol1}(y,t)+R_{rtv1})V_{ap}}{R_{pol1}R_{rtv1}C_{y1}} \\ 0 \end{bmatrix} \tag{29}$$

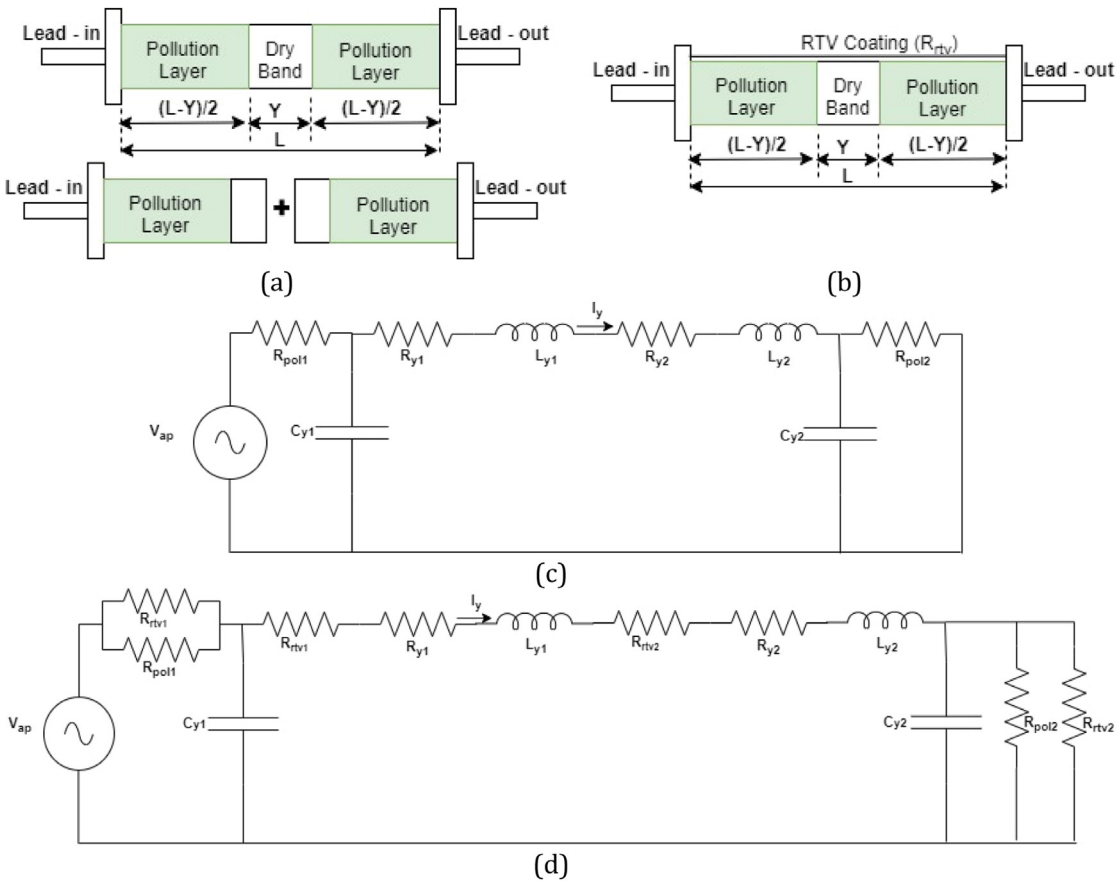

Fig. 3. Single dry band near middle region of HV bushing (a) without RTV coating (b) with RTV coating (c) Electrical equivalent circuit without RTV coating (d) Electrical equivalent circuit with RTV coating.

where $L_y=L_{y1}+L_{y2}, R_y=R_{y1}+R_{y2}$, $\frac{dR_{y1}}{dt}=\frac{R_{y1}}{\tau}(1-\frac{R_{y1}I_{y1}^2}{A})$, $\frac{dR_{y2}}{dt}=\frac{R_{y2}}{\tau}(1-\frac{R_{y2}I_{y2}^2}{A})$, $L_{y1}=\frac{\mu_0}{2\pi}(0.25+\ln(\frac{y_1}{r_{d1}}))$, $L_{y2}=\frac{\mu_0}{2\pi}(0.25+\ln(\frac{y_2}{r_{d2}}))$, $C_{y1}=2\pi\varepsilon\alpha_1[1+(\frac{r_{d1}}{L-y_1})]$, and $C_{y2}=2\pi\varepsilon\alpha_2[1+(\frac{r_{d2}}{L-y_2})]$.

As it is represented using two arc model, suffix 1 and 2 represents the lead-out and lead-in portion of HV bushing. Eqs. (30) and (31) are used to find the resistance of RTV coating bushing for narrow band equation and for wide band it is determined using Eqs. (32) and (33).

For Narrow band:

$$R_{pol1}=\frac{1}{2\pi\sigma}\left[\frac{\pi(L-y_1)}{w}+\log\left(\frac{w}{2\pi r_{d1}}\right)\right] \tag{30}$$

$$R_{pol2}=\frac{1}{2\pi\sigma}\left[\frac{\pi(L-y_2)}{w}+\log\left(\frac{w}{2\pi r_{d2}}\right)\right] \tag{31}$$

For Wide band:

$$R_{pol1}=\frac{1}{2\pi\sigma}\left(\log\frac{2L}{\pi r_{d1}}-\log\tan\frac{\pi y_1}{2L}\right) \tag{32}$$

$$R_{pol2}=\frac{1}{2\pi\sigma}\left(\log\frac{2L}{\pi r_{d2}}-\log\tan\frac{\pi y_2}{2L}\right) \tag{33}$$

Flow chart of proposed work and experimental work

The proposed work methodology is explained in Fig. 4. 22 kV bushing is used in this work and dry band location is varied in three different locations like lead in, lead out, and in the middle portion. Then, the proposed work is alienated into two segments. In

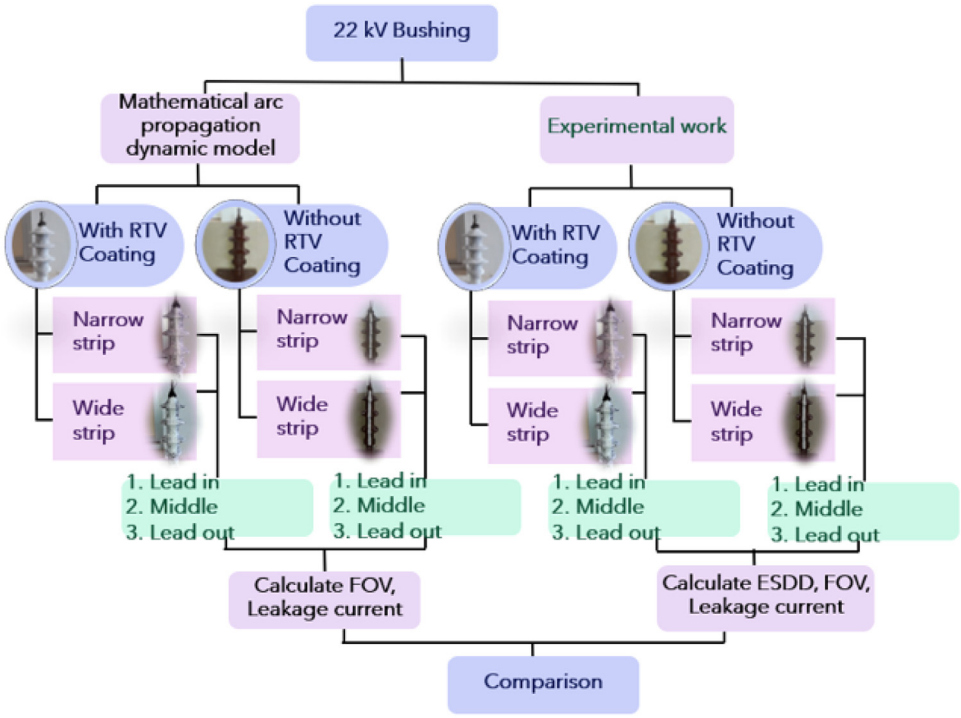

Fig. 4. Proposed methodology.

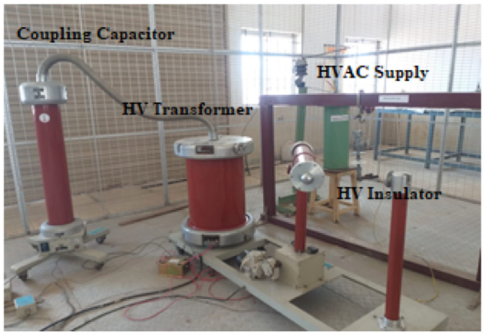

Fig. 5. Experimental setup.

the segment one, mathematical modeling work is carried out and FOV, leakage current was predicted for different y/L ratio. In the second section, experimental work is carried out for the same y/L ratio. The results were discussed and compared. The performance of the bushing is analyzed with and without RTV coating.

Experimental work

The climatic and meteorological factors that lead to flashover on contaminated bushings have a major impact on the reliability of power systems [35,36]. This causes system failures. In order to evaluate the bushings before employing them in a service, artificial pollution is applied [37]. In this proposed work, artificial RTV is coated on the high-voltage bushing surface. The experimental arrangement is displayed in Fig. 5

Test specimen

In this work, 22 kV bushing is taken as a test sample and artificial pollution is applied on the bushing with and without RTV coating on the bushing surface. Fig. 6 shows the bushing taken for this work with and without RTV coating.

Fig. 6. (a) HV bushing without RTV coating on the surface (b) HV bushing with RTV coating on the surface.

Artificial pollution on bushing

The test sample is washed with normal water, followed by distilled water. It is then cleaned with cotton. After that disodium phosphate is applied to the bushing samples to remove unseen dust particles present on the surface of the bushing. Then RTV coating is done on the sample. A mixture of 20 gm sodium chloride, 5 gm kaolin and 20 ml distilled water are used for artificial pollution and it is applied by following solid layer method. The brushing method, as opposed to dipping or spraying, has been employed in this study to apply pollution. It is crucial to use a dynamic approach, in which a model is based on the physical processes that make up the phenomena, to construct a realistic arc model. In MATLAB, the suggested approach is used to compute flashover voltage. The flowchart of arc propagation criteria and flashover voltage computation is described in Fig. 7. In this proposed work, Wilkins propagation criteria is used, which tries to extract maximum energy from source.

ESDD measurement

By using ESDD, pollutant severity is determined. Following testing, a little quantity of pollution layer is scraped off the bushing's surface, mixed in water for 30 to 40 min, and the solution's temperature is recorded. IEC 60507:2013 is appropriate for the purpose of the AC withstand characteristics of HV Bushing. Then, using IEC standard 60507, volume conductivity at a temperature of 200 °C is determined using (34).

$$s_{20} = s_{\theta}[1 - a(\theta - 20)] \tag{34}$$

Where θ is the solution temperature (C), and a is the influence contingents is calculated using Eq. (35).

$$b = -3.200 \times 10^{-8}(\theta)^3 + 1.032 \times 10^{-5}(\theta)^2 - 8.272 \times 10^{-4}(\theta) + 3.544 \times 10^{-2} \tag{35}$$

The salinity of the pollution (Sa) is calculated using the Eq. (36).

$$S_a = (5.7\sigma_{20})^{1.03} kg/m3 \tag{36}$$

ESSD is then calculated using salinity and area using the Eq. (37).

$$ESDD = S_a \times \frac{v}{A} mg/cm^2 \tag{37}$$

where V is the volume of solution(cm^3) and A is the area in the bushing surface corresponding to the pollution sample taken out (cm^2).

Investigational arrangement

Fig. 8(a) depicts the experimental setup used to measure flashover in bushings without RTV coating, while Fig. 8(b) depicts the experimental setup for measuring flashover in bushings with RTV coating. An HV transformer, a capacitance voltage divider, and a high voltage test specimen bushing make up the experimental setup. Control of the HV supply is done via the control panel. In this proposed FOV is calculated using even rising method and leakage current is measured at the instant of HV discharge take place in the bushing. In HV laboratory, initially the input supply is given to the HV coupling capacitor of rating 10,000 pF with the voltage rating of 144 kV. Next to that, there is a HV transformer of rating 120/3 kV and rated current of 2 × 22.8/0.1 A. At last, testing bushing is connected for testing with and without RTV coating for verification of mathematically derived breakdown voltage. The experimental test is conducted 10 times sequentially and the average value will be considered as a breakdown voltage.

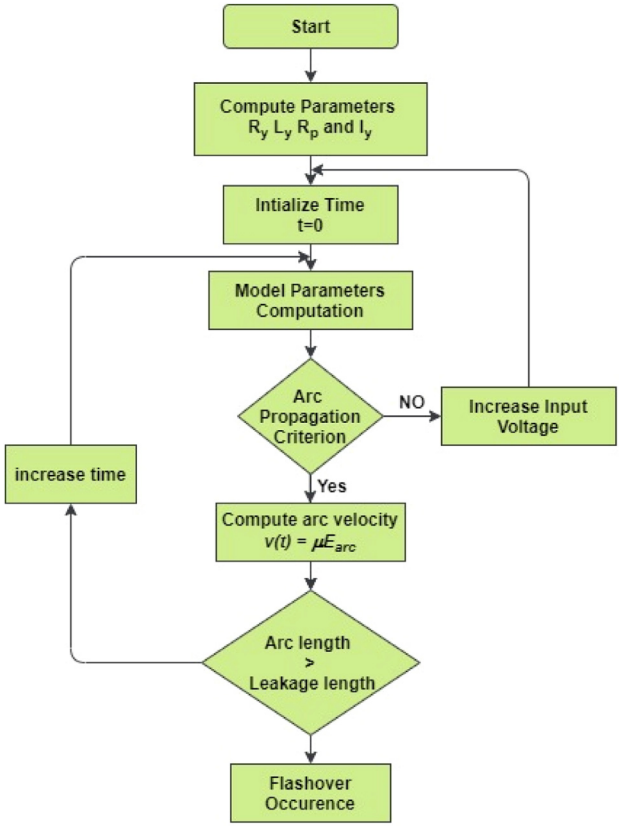

Fig. 7. Mathematical Arc propagation dynamic model.

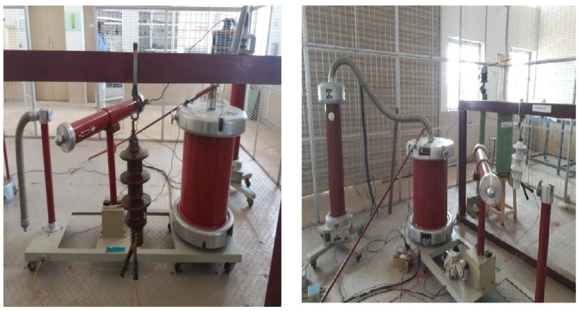

Fig. 8. Flashover measurement of polluted bushing (a)Without RTV coating (b) with RTV coating.

Results and discussion

The pollution performance of single dry band near lead-in region, middle region, and lead-out region of 22 kV bushing is analyzed for narrow and wide pollution band using FOV and discharge current. FOV and discharge current are predicted using mathematical modeling for different y/L ratio. For measuring the effectiveness of Mathematical modeling, predicted FOV and discharge current are verified with the experimental results obtained in high voltage laboratory. The width of dry band for narrow and wide band is quoted manually in the HV laboratory with dimension as mentioned in the Table 1.

Mathematical results

Flashover voltage and leakage current for both narrow and wide pollution band are estimated from the mathematical model of a single dry band located at the lead-in region, middle region, and lead-out region of 22 kV bushing. Table 1 shows the performance

Table 1
Mathematical results of FOV and Discharge current for single dry band at lead-in region of HV bushing.

S. No.	y/L Ratio	Discharge current (mA)		Flashover Voltage (kV)		Discharge current (mA)		Flashover Voltage (kV)	
		Narrow band Without RTV coating	Wide band	Narrow band	Wide band	Narrow band with RTV coating	Wide band	Narrow band	Wide band
1	0.2	2.76	30.40	12.11	13.19	18.64	19.79	20.92	21.22
2	0.3	3.16	34.13	12.18	14.01	20.35	21.32	29.49	29.88
3	0.4	3.78	38.20	12.29	14.99	22.53	23.75	36.99	37.31
4	0.5	4.67	42.70	12.46	16.20	25.45	27.31	43.30	43.54
5	0.6	6.02	47.50	12.71	17.59	29.33	31.54	47.15	47.28
6	0.7	8.80	54.12	13.21	19.43	30.95	33.25	51.28	51.98
7	0.8	15.8	61.60	14.49	21.68	32.52	34.75	53.30	54.95

Table 2
Mathematical results of FOV and Discharge current for single dry band at lead-out region of HV bushing.

S. No.	y/L Ratio	Discharge current (mA)		Flashover Voltage (kV)		Discharge current (mA)		Flashover Voltage (kV)	
		Narrow band Without RTV coating	Wide band	Narrow band	Wide band	Narrow band with RTV coating	Wide band	Narrow band	Wide band
1	0.2	2.74	30.30	24.14	25.17	0.2	24.79	26.69	59.14
2	0.3	3.17	34.14	24.22	26.01	0.3	25.55	29.71	60.92
3	0.4	3.78	38.20	24.29	26.98	0.4	29.37	32.13	62.49
4	0.5	4.68	42.21	24.49	28.21	0.5	33.53	35.42	65.33
5	0.6	6.06	47.76	24.87	29.74	0.6	37.44	37.79	68.91
6	0.7	8.80	54.39	25.18	31.49	0.7	39.95	43.58	70.03
7	0.8	15.80	61.80	26.43	33.79	0.8	42.51	45.32	72.25

Table 3
Mathematical results of FOV and Discharge current for single dry band at middle region of HV bushing.

S. No.	y/L Ratio	Discharge current (mA)		Flashover Voltage (kV)		Discharge current (mA)		Flashover Voltage (kV)	
		Narrow band Without RTV coating	Wide band	Narrow band	Wide band	Narrow band with RTV coating	Wide band	Narrow band	Wide band
1	0.2	1.20	13.00	24.01	24.41	53.3	57.8	111.4	117.2
2	0.3	1.28	14.00	24.03	24.70	57.2	60.1	117.9	121.9
3	0.4	1.36	14.60	24.05	25.14	61.9	62.5	123.2	129.5
4	0.5	1.40	16.06	23.59	25.95	65.2	67.9	109.6	113.7
5	0.6	1.50	17.10	23.50	26.03	69.1	71.3	112.4	130.5
6	0.7	1.70	17.23	24.21	26.37	72.7	77.9	133.5	141.9
7	0.8	1.90	19.00	24.34	26.95	75.3	79.3	138.3	145.4

of polluted bushing with and without RTV coating for different y/L ratios. The flashover voltage and discharge current increase with the increasing y/L ratios.

Both FOV and discharge current increase with an increase iny/L ratio for a narrow and wide band of the single dry band located near the lead-in region of RTV coated and non-coated HV bushing because increase in dry band length results in increase of resistance. For a single dry band located near the lead-out region, FOV and discharge current are calculated for RTV coated and non-coated HV bushing are tabulated in Table 2 for with and without RTV coating.

For increasing y/L ratios, FOV and discharge current increases in lead-out region exhibit similar behavior like lead-in region. On comparing narrow and wide band of the single dry band for both lead-in and lead-out region, FOV and discharge is higher for wide band due to increase in insulation resistance. Similarly for a single dry band located at the middle region of HV bushing, FOV and discharge current are estimated for various y/L ratios and tabulated in Table 3.

FOV and discharge current increase with y/L ratio for narrow and wide band and magnitude for wide band dominates the narrow band pollution in HV bushing.

Experimental results

The test specimen of a single dry band located at the lead-in region of HV bushing, for narrow and wide band of 0.8 y/L ratio is shown in Fig. 9.

Table 4 contains the experimental findings and an analysis of the pollution performance of a 22 kV bushing with a single dry band close to the lead-in region of the narrow and wide band.

With an increase in discharge length in the HV bushing testing sample, the ESSD value decreases. FOV and discharge current are increasing with an increase in y/L ratio for HV bushing with and without RTV coating. The experimental values are found to be good

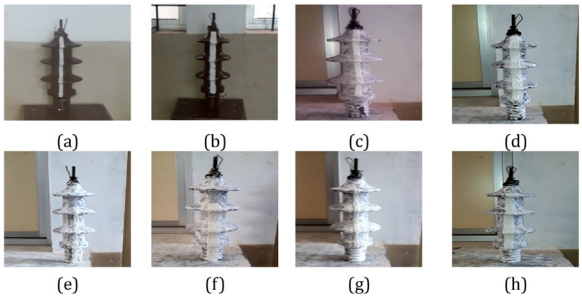

Fig. 9. Test specimen-22 kV bushing single dry band for 0.8 y/L ratio (a-b) without RTV coating, (c-h) with RTV coating (a-b) narrow and wide band near lead-in region, (c-d) narrow and wide band near lead-in region, (e-f) narrow and wide band near lead-out region, (g-h) narrow and wide band near middle region,.

Table 4
Experimental results of FOV and Discharge current for single dry band at lead-in region of HV bushing.

S. No.	y/L Ratio	Discharge current (mA)		Flashover Voltage (kV)		Discharge current (mA)		Flashover Voltage (kV)	
		Narrow band Without RTV coating	Wide band	Narrow band	Wide band	Narrow band with RTV coating	Wide band	Narrow band	Wide band
1	0.2	0.123	2.35	28.74	11.65	11.87	17.52	17.49	18.29
2	0.3	0.118	3.04	33.97	11.62	13.32	18.12	20.16	27.43
3	0.4	0.115	3.38	37.95	11.85	13.85	20.35	21.75	34.98
4	0.5	0.112	4.38	40.59	12.05	14.05	23.71	23.13	42.54
5	0.6	0.104	5.95	45.33	12.35	15.35	27.32	29.95	44.54
6	0.7	0.095	8.32	52.63	12.74	17.74	28.59	31.25	47.33
7	0.8	0.089	14.43	58.50	13.96	20.23	30.23	33.37	48.41

Table 5
Experimental results of FOV and Discharge current for single dry band at lead-out region of HV bushing.

S. No.	y/L Ratio	Discharge current (mA)		Flashover Voltage (kV)		Discharge current (mA)		Flashover Voltage (kV)	
		Narrow band Without RTV coating	Wide band	Narrow band	Wide band	Narrow band with RTV coating	Wide band	Narrow band	Wide band
1	0.2	0.123	2.55	28.03	22.15	23.65	22.36	24.59	57.22
2	0.3	0.118	2.89	31.99	21.56	24.88	23.73	25.73	58.45
3	0.4	0.115	3.52	37.27	22.31	25.62	27.15	27.18	60.12
4	0.5	0.112	4.33	41.22	22.98	27.01	29.23	33.56	63.22
5	0.6	0.104	5.86	45.89	22.55	28.41	34.32	34.79	66.98
6	0.7	0.095	7.89	51.68	23.23	29.55	37.51	40.18	68.04
7	0.8	0.089	13.99	58.33	24.12	31.66	41.15	42.38	71.89

degree proximity with mathematical results. Experimental readings of FOV and discharge current of 22 kV bushing with the single dry band near the lead-out region of narrow and wide band are shown in Table 5.

The ESSD value drops as the discharge length lengthens, but the FOV and discharge current lengthen as well. With an increase in ESDD values, the FOV and discharge current magnitudes decrease. The wide band's FOV and discharge current are larger than those of the narrow band. The pollution performance of a 22 kV bushing with a single dry band in the midst of the narrow and wide band is displayed in Table 6.

With an increase in discharge length, the ESSD value decreases but FOV and discharge current increases. Both the mathematical and experimental results of the single dry band of the HV bushing at different locations are found to be in close agreement. As a result, the mathematical model is created for the single dry band at various bushing locations. Each time the discharge length was extended, the ESSD value decreased, while the FOV and discharge current increased. Increased discharge length causes flashover to fully extend, the resistive component leakage current to be the only one present, increasing the leakage current and (FOV). The concordance between measured and calculated values of FOV and discharge current is shown in Fig. 10. The measured results are slightly lower than calculated. This is due to temperature rise, stochastic nature of flashover process, unassured uniform pollution coating (after having great effort), discharge width role and vertical electrical field stress component.

In bushing, the flashover process takes the form of sliding discharge as the electric field has a high-stress normal component acting on the bushing surface. When flashover develops, the magnitude is characterized by inductance, arc resistance, and pollution resistance connected in series whereas when the flashover gets fully elongated, this leakage current has resistive component current alone. With increase in ESDD, both FOV and discharge current decreases. With high ESDD, it facilitates the discharge current flow resulting in high magnitude FOV and discharge current. Moreover, the mathematical values are slightly higher than experimental

Table 6
Experimental results of FOV and Discharge current for single dry band at middle region of HV bushing.

S. No.	y/L Ratio	Discharge current (mA)		Flashover Voltage (kV)		Discharge current (mA)		Flashover Voltage (kV)	
		Narrow band Without RTV coating	Wide band	Narrow band	Wide band	Narrow band with RTV coating	Wide band	Narrow band	Wide band
1	0.2	0.123	1.15	11.55	23.28	23.56	51.2	55.2	105.3
2	0.3	0.118	1.02	12.32	22.15	22.23	55.2	58.2	109.2
3	0.4	0.115	1.22	13.89	23.42	23.55	58.4	60.5	110.5
4	0.5	0.112	1.31	14.22	21.22	24.26	61.2	65.6	105.4
5	0.6	0.104	1.42	15.36	21.85	25.98	67.6	71.4	110.2
6	0.7	0.095	1.67	15.89	22.36	25.42	71.4	75.2	128.8
7	0.8	0.089	1.78	17.22	22.85	25.02	73.2	78.4	130.3

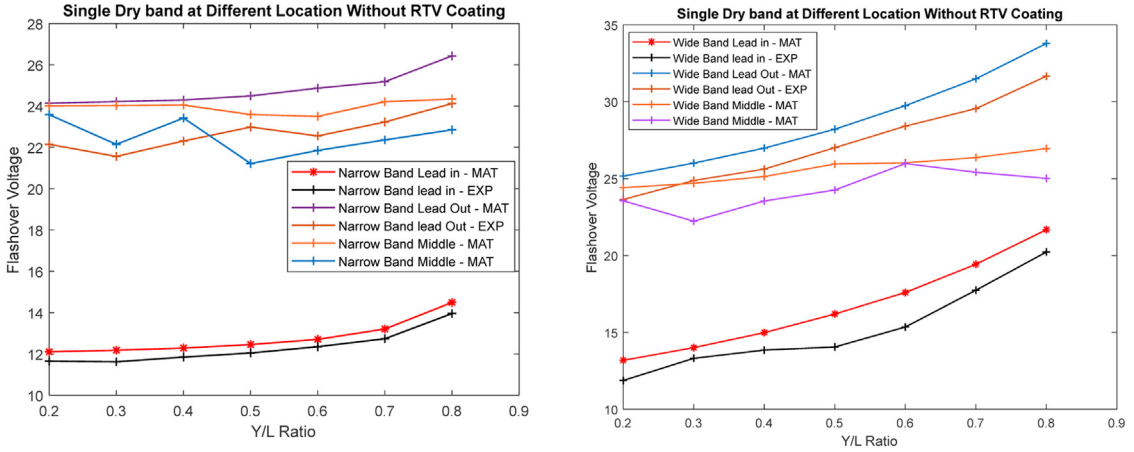

Fig. 10. Comparison of FOV for narrow and wide pollution band without RTV coating (a) Narrow (b) Wide (Mathematical Model and Experimental).

results as an increase in temperature, ESDD values, slight non-uniform pollution coating despite great effort, vertical electric field stress component are not accounted in the proposed dynamic model. Besides, the unique characteristics of experimental determination is also an added reason for the deviation in results.

Conclusion

The proposed bushing model developed for the single dry band at different locations namely lead-in, lead-out and middle region. This model is used to characterize the discharge propagation process leading to flashover for AC voltages. Hence it aids in enumerating the characteristic parameters which will tend to give a high flashover voltage. The mathematical model predicted the FOV and discharge current for dry band location at lead-in, lead-out, and middle region of the contaminated bushing with and without RTV coating. The influence of dry band location in HV bushing on flashover voltage is studied for different y/L ratios, dry band locations and ESDD. The predicted flashover voltage and leakage current from the mathematical model for HV bushing for different dry band locations are found to have a good degree of agreement with experimental values for HV bushing for different dry band locations.

Ethics statements

The authors state that the work did not involve any data collected from social media platforms.

Declaration of competing interests

The authors declare that they have no known competing financial interests or personal relationships that could have appeared to influence the work reported in this paper.

CRediT authorship contribution statement

L. Kalaivani: Conceptualization, Methodology. **R.V. Maheswari:** Conceptualization, Methodology. **Emad Makki:** Methodology, Formal analysis, Validation, Writing – review & editing. **Sanjay B Warkad:** Validation, Formal analysis, Writing – original draft. **B. Vigneshwaran:** Conceptualization, Methodology. **Alagar karthick:** Validation, Formal analysis, Writing – original draft. **Hitesh Panchal:** Validation, Formal analysis, Writing – original draft.

Data availability

Data will be made available on request.

References

[1] T. Chihani, A. Mekhaldi, A. Beroual, M Teguar, D. andMadjoudi, Model for pollutedinsulator flashover under AC or DC Voltage, IEEE Trans. Dielectr. Electr. Insul. 25 (2) (2018) 614–622.
[2] Y. Yan, W. Jiang, A. Zhang, Q.M. Li, H.J. Li, W. Chen, Y. Lei, Research on configuration design and operation effect evaluation for ultra high voltage vertical insulator cleaning robot, Industr. Robot 47 (1) (2019) 90–101.
[3] X. Xu, Y. Nie, X. Peng, Research on insulation detection of insulator strings with fuzzy logical reasoning method, Kybernetes 38 (10) (2009) 1747–1753.
[4] K. Aramugam, H.A. Illias, Y.C. Ching, Optimisation of corona ring design for composite insulator strings, COMPEL - Int. J. Comput. Math. Electr. Electron. Eng. 38 (1) (2019) 232–246.
[5] M. KouhiJemsi, B. Vahidi, R. Naghizadeh, S. HosseinHosseinian, Optimum design of high voltage bushings by rational Bézier curves, COMPEL - Int. J. Comput. Math. Electr. Electron. Eng. 31 (6) (2012) 1901–1916.
[6] E. Kuffel, W.S. Zaengl, J Kuffel, High Voltage Engineering, Second edition, Butterworth-Heinemann, 2000.
[7] W.H. Schwardt, J.P. HoltZhausen, W.L Vosllo, A comparison between measured leakage current and surface conductivity during salt fog tests, in: October 2004, AFRICON Conference, 2014, pp. 597–600.
[8] Zhijin Zhang, Xiaohuan Liu, Xingliang Jiang, Jianlin Hu, David WenzhongGao, Study on AC flashover performance for different types of porcelain and glass insulators with non-uniform pollution, IEEE Trans. Power Deliv. 28 (3) (2013) 1691–1698.
[9] A. Arshad, Nekahi, S.G. McMeekin, et al., Measurement of surface resistance of silicone rubber sheets under polluted and dry band conditions, Electr. Eng. 100 (2018) 1729–1738, doi:10.1007/s00202-017-0652-x.
[10] A. Arshad, Nekahi, S.G. McMeekin, et al., Effect of pollution severity and dry band location on the flashover characteristics of silicone rubber surfaces, Electr. Eng. 99 (2017) 1053–1063, doi:10.1007/s00202-016-0473-3.
[11] Muhammad Ali Arshad, Azam Mughal, Mansoor khan Nekahi, Farhana Umer, Influences of single and multiple dry bands on critical flashover voltage of silicone rubber outdoor insulator: simulation and experimental study, Energies 11 (2018) 1335.
[12] K. Naito, G. Ramos, M.T Campillo, A study on the characteristics of various conductive contaminants accumulated on high voltage insulators, IEEE Trans. Power Deliv. 8 (4) (1993) 1842–1850.
[13] G.N. Ramos, M.T.R. Campillo, K Naito, A study on the characteristics of various conductive contaminants accumulated on high voltage insulators, IEEE Trans. Power Del. 8 (1993) 1842–1850.
[14] Y.A. Bencherif, A. Mekhaldi, J. Lobry, et al., Multiscale analysis of the polymeric insulators degradation in simulated arid environment conditions: cross-correlation assessment, J. Electr. Eng. Technol. 15 (2020) 135–146, doi:10.1007/s42835-019-00217-7.
[15] R. Matsuoka, H. Shinokubo, K. Kondo, Y. Mizuno, K. Naito, T. Fujimura, T Terada, Assessment of basic contamination withstand voltage characteristics of polymer insulators, IEEE Trans. Power Delv. 11 (1996) 1895–1900.
[16] H.G. Kim, H.C. Jung, J.D. Park, et al., Measurement of sheet-like space charge distribution and signal calibration of insulator XLPE Using PEA method, J. Electr. Eng. Technol. 15 (2020) 2027–2032, doi:10.1007/s42835-020-00477-8.
[17] C. Volat, M. Farzaneh, N. Mhaguen, Improved FEM models of one andtwo arcs to predict AC critical flashover voltage of ice-covered insulators, IEEE Trans. Dielectr. Electr. Insul. 18 (2) (2011) 393–400.
[18] Chuyan Zhang, Liming Wang, Zhicheng Guan, Pollution flashover performance of full-scale ±800 kV converter station post insulators at high altitude area, IEEE Trans. Dielectr. Electr. Insul. 20 (3) (2013) 717–726.
[19] E.A. Cherney, A. El-Hag, S.Li.R.S Gorur, L. Meyer, I. Ramirez, M. Marzinotto, J.M. George, RTV silicone rubber pre-coated ceramic insulators for transmission lines, IEEE Trans. Dielectr. Electr. Insul. 20 (1) (2013) 237–244.
[20] R.T. Waters, A. Haddad, H. Griffiths, N. Harid, P. Sarkar, Partial arc spark models of the flashover of the lightly polluted insulators, IEEE Trans. Dielectr. Electr. Insul. 17 (2010) 417–424.
[21] A. Arshad, Nekahi, S.G. McMeekin, M. Farzhaneh, Flashover characteristics of silicone rubber sheets under various environmental conditions, Energies 9 (2016) 683.
[22] F.A.M. Rizk, Mathematical models for pollution flashover, Electra 78 (1981) 71–103.
[23] A. Banik, A. Mukherjee, S. Dalai, Development of a pollution flashover model for 11 kV porcelain and silicon rubber insulator by using COMSOL multiphysics, ElectrEng 100 (2018) 533–541.
[24] R Wilkins, Flashover voltage of high voltage insulators with uniform surface pollution films, Proc. IEEE 116 (3) (1969).
[25] F. Obenaus, Fremdschicht, 'Uberschlag und Kriechweglange', Deut. Electrotech. 2 (4) (1958) 135–136.
[26] D.C. Jolly, Contamination flashover, part I:theoritical aspects, IEEE Trans. Power Appar. Syst. PAS-91 (1972) 2437–2442.
[27] C.S. Engelbrecht, Ralf Hartings, Helena Tunell, Bjorn Engstrom, Harald Janssen, Raimund Hennings, Pollution tests for coastal conditions on an 800-kV Composite Bushing, IEEE Trans. Power Deliv. 18 (3) (2003) 953–959.
[28] R.V. Maheswari, B. Vigneshwaran, L. Kalaivani, Genetic algorithm based automated threshold estimation in translation invariant wavelet transform for denoising PD signal, COMPEL - Int. J. Comput. Math. Electr. Electron. Eng. 34 (4) (2015) 1252–1269.
[29] I. Fofana, A. Beroual, A new proposal for calculation of the leader velocity based on energy considerations, J. Phys. D: Appl. Phys. 29 (1996) 691–696.
[30] O. Mayer, BeitragzurTheorie der Statischen und der DynamishchenLitchbogens, Arch. Elektrotechnik (Vol.37) (1943) 588–608.
[31] R. Sundararajan, R.S Gorur, Dynamic arc modeling of pollution flashover of insulators under dc voltage, IEEE Trans. Electr. Insul. 28 (1993) 209–218.
[32] N. Dhahbi-Megriche, A. Beroual, Flashover dynamic model of polluted insulators under ac voltage, IEEE TDEI 7 (2) (2000) 283–289.
[33] C. Tavakoli, M. Farzaneh, I. Fofana, et al., Dynamics and modeling of AC arc on surface of ice, IEEe Trans. Dielectr. Electr. Insul. 13 (6) (2006) 1278–1285.
[34] I. Fofana, A. Beroual, Predischarge models in dielectric liquids, Jpn. J. Appl. Phys. 37 (1998) 2540.
[35] H.I. Uckol, B.I. Karaca, S.D.C and, AC electric field analysis and experimental verification of a silicone rubber insulator, ElectrEng 102 (2020) 503–514, doi:10.1007/s00202-020-00954-3.
[36] M. Natarajan, V. Basharan, K.G. Pillai, M.R. Velayutham, W.I.M. Silluvairaj, Analysis of stress control on 33-kV non-ceramic insulators using finite-element method, Electr. Power Components Syst. 43 (5) (2015) 566–577.
[37] H. Mohseni, A.N. Jahoemi, M.S. Pasand, S.H. Jayaram, A.A.S. Akmal, A Method of increment short- circuit current in test of ceramic and composite polluted insulators, IEEE Trans. Power Deliv. 22 (2007) 977–985.